Uptake and Cytotoxicity of Chitosan Molecules and Nanoparticles: Effects of Molecular Weight and Degree of Deacetylation

Min Huang,[1] Eugene Khor,[2] and Lee-Yong Lim[1,3]

Received August 25, 2003; accepted October 25, 2003

Purpose. To evaluate the effects of molecular weight (Mw) and degree of deacetylation (DD) on the cellular uptake and *in vitro* cytotoxicity of chitosan molecules and nanoparticles.

Methods. Chemical depolymerization and reacetylation produced chitosans of Mw 213,000 to 10,000 and DD 88-46%, respectively. Chitosan was labeled with FITC and transformed into nanoparticles by ionotropic gelation. Uptake of chitosan by confluent A549 cells was quantified by fluorometry, and *in vitro* cytotoxicity was evaluated by the MTT and neutral red uptake assays.

Results. Nanoparticle uptake was a saturable event for all chitosan samples, with the binding affinity and uptake capacity decreasing with decreasing polymer Mw and DD. Uptake fell by 26% when Mw was decreased from 213,000 to 10,000, and by 41% when DD was lowered from 88% to 46%; the uptake data correlated with the ζ potential of the nanoparticles. Uptake of chitosan molecules did not exhibit saturation kinetics and was less dependent on Mw and DD. Postuptake quenching with trypan blue indicated that the cell-associated chitosan nanoparticles were internalized, but not the cell-associated chitosan molecules. Chitosan molecules and nanoparticles exhibited comparable cytotoxicity, yielding similar IC_{50} and IC_{20} values when evaluated against the A549 cells. Cytotoxicity of both chitosan entities was attenuated by decreasing polymer DD but was less affected by a lowering in Mw.

Conclusions. Transforming chitosan into nanoparticles modified the mechanism of cellular uptake but did not change the cytotoxicity of the polymer toward A549 cells. Chitosan DD had a greater influence than Mw on the uptake and cytotoxicity of chitosan nanoparticles because of its effect on the ζ potential of the nanoparticles.

KEY WORDS: molecular weight; degree of deacetylation; chitosan; uptake; cytotoxicity.

INTRODUCTION

Chitosan, a polycationic polymer comprising of D-glucosamine and N-acetyl-D-glucosamine linked by β(1,4)-glycosidic bonds, has been exploited as a carrier for the delivery of anticancer drugs, genes, and vaccines (1–3). In these applications, it is important to assess the effectiveness of uptake of the carrier and associated drug cargo into the target cells. We have quantified the cellular uptake of chitosan by fluorimetric techniques (4,5) and found that the transformation of chitosan into nanoparticles facilitated its internalization by absorptive cells. However, only one chitosan sample with molecular weight (Mw) of 180 kDa and degree of deacetylation (DD) of 90% was evaluated, whereas chitosans of a wide range of Mw and DD have been applied to drug delivery. Because the physical and biologic properties of chitosan are dependent on its Mw and DD (6,7), the present study set out to evaluate the effects of these two parameters on the cellular uptake of chitosan.

Another objective of the present study was to correlate the uptake of chitosan to its cytotoxicity. Chitosan, being a natural polymer, has been widely regarded as biocompatible. Indeed, chitosan has been shown to be degraded *in vivo* by enzymes, such as lysozyme and chitosanase, into oligomers and further to N-glucosamine, which is endogenous to the human body (8). However, the term "biocompatible" can be misleading if the polymer is not evaluated in relation to its structural parameters, its dosage form, the intended use, and the route of administration (9). Moreover, there is evidence that certain chitosan samples were hemolytic (10) and should not be classified as inert carriers. Of the factors that determined the biocompatibility of chitosan, Mw and DD again emerged to be critical. Tomihata *et al*. have found that chitosans with DD below 70% were readily degraded when implanted subcutaneously in rats, whereas chitosans with DD above 70% were poorly degraded (11). This difference in biodegradation profile bordering the 70% DD mark was attributed to the sequential arrangement of the N-acetylglucosamine units necessary for identification by the chitosan-degrading enzymes. The results were corroborated by another study in which chitosans with relatively low Mw of 4.65×10^5 or relatively low DD of 76.0% were found more susceptible to degradation by β-glucosidase compared to chitosans with Mw of 10.6×10^5 or DD of 92.4% (12). Despite the association of high Mw and DD to the cytotoxic and hemolytic properties of chitosan (10,13,14), a systematic study on the effects of Mw and DD on the cytotoxicity of chitosan has not been reported. Neither has the cytotoxicity of chitosan nanoparticles been evaluated as a function of the Mw and DD of the polymer.

The objectives of the present study were to determine the effects of Mw and DD on the uptake and cytotoxicity of chitosan presented as soluble molecules and condensed nanoparticles. Chitosans of defined Mw and DD were prepared from a commercial chitosan sample by chemical depolymerization (15) and reacetylation with acetic anhydride (16), respectively. To visualize and quantify the cell-associated chitosan, the chitosan was conjugated with fluorescein-5-isothiocyanate before the uptake experiments (4,5). Chitosan was transformed into nanoparticles by ionotropic gelation with tripolyphosphate ions (17) and characterized for size, size distribution, and ζ potential. Uptake and cytotoxicity studies were performed on confluent A549 cells, a human lung carcinoma cell line (18). The MTT (19) and neutral red uptake (20) assays were used to measure the *in vitro* cytotoxicity of chitosan.

MATERIALS AND METHODS

Materials

Chitosan (Aldrich Chemical Co., Milwaukee, WI), pentasodium tripolyphosphate (TPP) (Darmstadt, Germany), and sodium nitrite ($NaNO_2$) (Nacailai Tesque, Japan) were

[1] Department of Pharmacy, National University of Singapore, 18 Science Drive 4, Singapore 117543.
[2] Department of Chemistry, National University of Singapore, 18 Science Drive 4, Singapore 117543.
[3] To whom correspondence should be addressed (email: phalimly@nus.edu.sg).

0724-8741/04/0200-0344/0 © 2004 Plenum Publishing Corporation

used as received. Other materials consisted of CH_3COOH, acetic anhydride, methanol, 3-(4,5-dimethylthiazol-2-yl)-2,5-diphenyltetrazolium bromide (MTT) from BDH Chemicals Ltd. (Poole, England); 20 × SSC medium (containing 3 M NaCl, 0.3 M sodium citrate, pH 7.0) from Molecular Probes (Eugene, OR, USA); and fluorescein-5-isothiocyanate (FITC), NaOH, neutral red, Triton X-100 from the Sigma Chemical Co. (St. Louis, MO, USA). The transport medium consisted of Hanks Balanced Salt Solution (HBSS, Sigma) buffered with 10 mM N-2-hydroxyethylpiperazine-N′-2-ethanosulfonic acid (HEPES, Sigma) and adjusted to pH 6.2 with 1 M HCl (Sigma). Ultrapure water (Millipore, Bedford, MA, USA) was used. Other chemicals were of the highest grade available commercially.

A549 cells (Passage 80) from the American Type Culture Collection (ATCC) were cultured in Ham's F12-K medium (Sigma), supplemented with 10% fetal bovine serum (Gibco BRL Life Technology, Grand Island, NY, USA), 100 μg/ml penicillin G (Sigma), and 100 μg/ml streptomycin sulfate (Sigma) at 37°C in a humidified 95% air/5% CO_2 environment (NuAire, Plymouth, MN, USA).

Synthesis and Characterization of Depolymerized and Reacetylated Chitosans

Chitosan (2% w/v in 6% v/v CH_3COOH, 100 ml) was depolymerized by chemical reaction for 1 h with 10 ml of $NaNO_2$ (0.5 to 20 mg/ml in water). The depolymerized chitosan was precipitated by raising the pH to 9 with 4 M NaOH, washed thoroughly with 70% methanol, dialyzed for 2 days against 5 L of distilled water, and freeze-dried (Dynavac, Auckland, New Zealand). For the synthesis of chitosan with lower DD, 750 mg of chitosan was reacted with 1.2 g of acetic anhydride in 80 ml of solvent (0.375% CH_3COOH/31.25% methanol) or with 0.4 g of acetic anhydride in 60 ml of solvent (0.5% CH_3COOH/41.67% methanol) at ambient temperature overnight. The reacetylated chitosan was precipitated by adjusting the pH of the solution to 7 with 1 M NaOH, washed extensively with water to neutrality, and freeze-dried. All syntheses were repeated three times.

The Mw of chitosan was determined in a gel permeation chromatogram (Waters, PL-GFC 8 μm, 7.6 × 300 mm columns) calibrated with pullulan standards (5.9–788 kDa, Shodex P-82, Showa Denko, Japan) using 0.333 M CH_3COOH/0.1 M CH_3COONa as the mobile phase (21). The flow rate was 0.8 ml/min. DD of chitosan was measured using the first derivative UV spectrometry method (22). Infrared spectra of the chitosan samples (2 mg + 198 mg KBr) were acquired using a Fourier transform infrared spectrophotometer (JASCO FT-IR, Japan).

Preparation and Characterization of FITC-Labeled Chitosan Nanoparticles

FITC-labeled chitosan was synthesized by adding 100 ml of dehydrated methanol followed by 50 ml of FITC in methanol (2.0 mg/ml) to 100 ml of chitosan (1% in 0.1M CH_3COOH) in the dark at ambient temperature. After 3 h, the labeled polymer was precipitated in 0.2 M NaOH. The precipitate was pelleted at 40,000 *g* (10 min) and washed with methanol:water (70:30, v/v). The washing and pelletization were repeated until no fluorescence was detected in the supernatant (Perkin-Elmer LS-5B luminescence spectrometer, Beaconsfield, England, λ_{exc} = 490 nm, λ_{emi} = 520 nm). The labeled chitosan was redissolved in 20 ml of 0.1 M HAc and dialyzed in the dark against 5 L of water for 3 days, the water being replaced with fresh water every 6 h. Finally, the labled chitosan was freeze-dried. Labeling efficiency (% w/w FITC to FITC-chitosan) was determined by measuring the fluorescence intensity of the FITC-chitosan solution against standard solutions of FITC (4,5).

Chitosan nanoparticles were prepared by ionotropic gelation of chitosan molecular chains with the polyanionic TPP ions at high speeds of agitation (17). Nanoparticles formed spontaneously when 4 ml of TPP (0.10% in water) solution was added gradually to 8 ml of chitosan (0.25% in 0.1 M CH_3COOH) with stirring at 1000 rpm (Corning Stirrer/Hot Plate) at ambient temperature. Chitosan molecules in solution were prepared in a similar manner by replacing the TPP solution with water. FITC-labeled chitosan nanoparticles and chitosan solution were similarly prepared with the labeled polymer. Nanoparticles were measured for size and ζ potential in a particle sizer (Zetasizer 3000, Malvern Instruments Ltd, Worcs, UK). The morphology of the nanoparticles was observed under a transmission electron microscope (TEM). Samples were stained with 2% of phosphotungstic acid and placed on copper grids with Formvar® films for viewing under the TEM (Jeol JEM-100CXII, Japan). All formulations were characterized immediately on preparation.

For ease of discussion, chitosan molecules and chitosan nanoparticles are abbreviated as CS and NP, respectively, and their corresponding FITC-labeled counterparts are designated as FCS and FNP.

Uptake of FITC-Chitosan Molecules and Nanoparticles by A549 Cells

A549 cells of passages 82–90 were plated in Multiwell 12-well plates at a density of 1.6×10^5 cells/cm^2 and used for uptake studies on days 4 and 5 on confluency. Dosing solutions consisted of freshly prepared FNP or FCS diluted with the transport medium to give equivalent chitosan concentrations of 0.2 to 1.0 mg/ml and adjusted to pH 6.2 with 1 M NaOH. Each cell monolayer was rinsed three times and preincubated with 1 ml of transport medium at 37°C. Uptake was initiated by exchanging the transport medium with 1 ml of specified dosing solution and incubating the cells at 37°C for 0.5 to 4 h. The experiment was terminated by washing the cell monolayer three times with ice-cold phosphate-buffered saline (PBS; 8 g/L NaCl, 0.2 g/L KCl, 1.44 g/L Na_2HPO_4, and 0.24 g/L KH_2PO_4 in water at pH 7.4) and solubilizing the cells with 1 ml of 0.5% Triton X-100 in 0.2 M NaOH. Cell-associated chitosan was quantified by analyzing the cell lysate in a fluorescence plate reader (Spectra Fluor, Tecan Group Ltd., Männedorf, Switzerland, λ_{exc} = 485 nm, λ_{emi} = 535 nm). Uptake was expressed as the amount (micrograms) of chitosan associated with a unit weight (1 mg) of cellular protein. The protein content of the cell lysate was measured using the Micro BCA protein assay kit (Pierce Chemical Company, Rockford, IL, USA).

The plate reader was calibrated with standard preparations of FNP and FCS, which were diluted with a cell lysate solution prepared by solubilizing 2×10^5 A549 cells in 1 ml of 0.5% Triton X-100/0.2 N NaOH solution. Linear calibration

curves ($R^2 \geq 0.99$) over the chitosan concentration range of 3.33 to 53.33 μg/ml were obtained for the FNP and FCS of each chitosan sample.

Confocal Microscopy

A549 cells of passage 88 were seeded onto Lab-Tek® chambered coverglass (Nalge Nunc International, Naperville, IL) at a density of 5×10^4 cells/cm^2 and cultured in 0.2 ml of Ham's F-12K at 37°C in the incubator. After 2 days of culture, the cell monolayers were washed twice and preincubated with 0.1 ml of prewarmed transport medium for 30 min at 37°C. Uptake was initiated by adding 0.1 ml of FNP or FCS into the medium (final chitosan concentration of 0.2 mg/ml). After 2 h of incubation at 37°C, the FNP or FCS was removed, and the cells were incubated with 0.2 ml of trypan blue (400 μg/ml in 0.1 M citrate buffer, pH 4.4) for 1 min before they are washed twice with prewarmed PBS solution, fixed in 3.7% paraformaldehyde for 10 min, and stained with propidium iodide (2 μg/ml in 2 × SSC containing 25 μg/ml RNase A) for 10 min. The specimens after storage overnight at 4°C in Jung® tissue-freezing medium (Leica Instruments, Germany) were examined under an inverted confocal microscope (CLSM, Zeiss Axiovert 200M, Oberkochen, Germany) equipped with a LSM 5 Image Browser (Carl Zeiss, Oberkochen, Germany).

In Vitro Cytotoxicity of Chitosan and Nanoparticles on A549 Cells

The determination of cell viability is a common assay to evaluate the *in vitro* cytotoxicity of biomaterials. In the present study, cell viability was assessed by the MTT (19) and neutral red uptake (20) assays. The MTT assay is a quantitative and rapid colorimetric method based on the cleavage of a yellow tetrazolium salt (MTT) to insoluble purple formazan crystals by the mitochondrial dehydrogenase of viable cells. Neutral red is a vital dye that is endocytosed by viable cells and internalized within lysosomes. The combination of these two different methods adds reliability to the final evaluation of cytotoxicity for the chitosan materials.

NP and CS samples were sterilized by UV irradiation overnight. A549 cells were seeded onto 96-well plates at a density of 10,000 cells/well and cultured in 100 μl of Ham's F-12K medium for 24 h in the CO_2 incubator. The spent medium was replaced with CS or NP and diluted with culture medium to give a chitosan concentration of 0.098 to 1.667 mg/ml (pH 6.2). After 4 h of incubation at 37°C, the CS and NP were replaced with 100 μl of MTT (0.5 mg/ml in HBSS, pH 7.4) or 150 μl of neutral red (1 mg/ml in HBSS, pH 7.4) solutions, and the cells incubated for a further 3 h at 37°C. The test solution was decanted, and 150 μl of DMSO (MTT assay) or destaining solution (neutral red assay; comprising 1:50:49 v/v of glacial acetic acid/ethanol/water) was added to solubilize the cells. The resultant solutions were measured in a microplate reader (Molecular Devices Corporation, Palo Alto, CA, USA) at λ_{590} (MTT assay) or λ_{540} (neutral red assay). Cell viability was expressed as percentage of absorbance relative to control, the control comprising cells not exposed to the chitosan materials. Experiments were performed in triplicates, with eight replicate wells for each sample and control per assay. The IC_{50} and IC_{20}, representing the respective concentrations at which 50% and 20% of cell growth were inhibited, were calculated and expressed as mean ± SD.

Statistical Analyses

Results are expressed as means ± SD. Uptake data were analyzed by one-way ANOVA with the *post-hoc* Tukey's test applied for paired comparisons ($p = 0.05$) (SPSS 10, SPSS Inc., Chicago, IL, USA).

RESULTS

Effect of Mw and DD on the Uptake of FNP and FCS by A549 Cells

The commercial chitosan had Mw of 213 ± 6 kDa and DD of 88.0 ± 0.5% ($n = 3$). Depolymerization with $NaNO_2$ produced chitosans with Mw of 98 ± 6 kDa (400:1 w/w of chitosan:$NaNO_2$), 48 ± 4 kDa (80:1), 17 ± 2 kDa (20:1), and 10 ± 2 kDa (10:1). The polydispersity (Mw/Mn) of the samples fell from 2.64 for the parent polymer to 1.17 for the 10-kDa sample, indicating increasingly monodispersed chain lengths. DD (Fig. 1a) and FTIR spectra (Fig. 2) were not affected by the depolymerization process. Reacetylation with acetic anhydride produced chitosans with lower DD of 61 ± 4.6% (1.875:1 w/w of chitosan:acetic anhydride) and 46 ± 1.1% (0.625:1) without modifying the Mw (Fig. 1b). FTIR spectra for the reacetylated samples showed a more prominent amide II band at 1560 cm^{-1} and well-differentiated amide I (1650 cm^{-1}) and amide II (1560 cm^{-1}) bands, which were consistent with the higher acetyl content of the samples (Fig. 2). In contrast, the -NH_2 band at 1590 cm^{-1} obscured the amide II band at 1560 cm^{-1} for the commercial chitosan, which had a higher DD of 88% (Fig. 2). To differentiate among chitosan samples, the abbreviation M*m*D*n* will be used, where *m* represents the Mw of the polymer (in thousands), and *n* the DD (in percent).

Size and ζ potential of the chitosan nanoparticles (NP) were dependent on the chitosan Mw and DD (Table I). Lowering the Mw from 213 to 17 kDa caused the mean particle size to fall from 188 to 122 nm, although further reduction of the Mw to 10 kDa reversed the trend, and the mean size of NP-M10D88 was increased to 265 nm. None of the NP batches showed particle aggregation under the TEM (results not shown), including the NP-M10D88. The ζ potential fell from 34.6 mV for NP-M213D88 to 25.4 mV for NP-M10D88. A larger difference in ζ potential (20.3 mV) was observed between NP-M213D88 and its reacetylated counterpart, NP-M213D46. The reacetylated chitosans also yielded NP of larger mean size than the parent polymer.

All the chitosan samples were successfully labeled with FITC, the labeling efficiency ranging from 2.3 to 8.6%w/w, with higher efficiency obtained for samples with lower Mw or DD (Table I). Paired *t* test analyses of the data suggested that the FITC-conjugation did not change the ζ potential of the chitosan nanoparticles (Table I), but it significantly modified the mean size of nanoparticles prepared with the parent and depolymerized chitosan samples. However, despite the statistically significant differences in mean size among the various NP and FNP samples, it should be noted that these formulations had relatively wide size distribution (polydispersity >

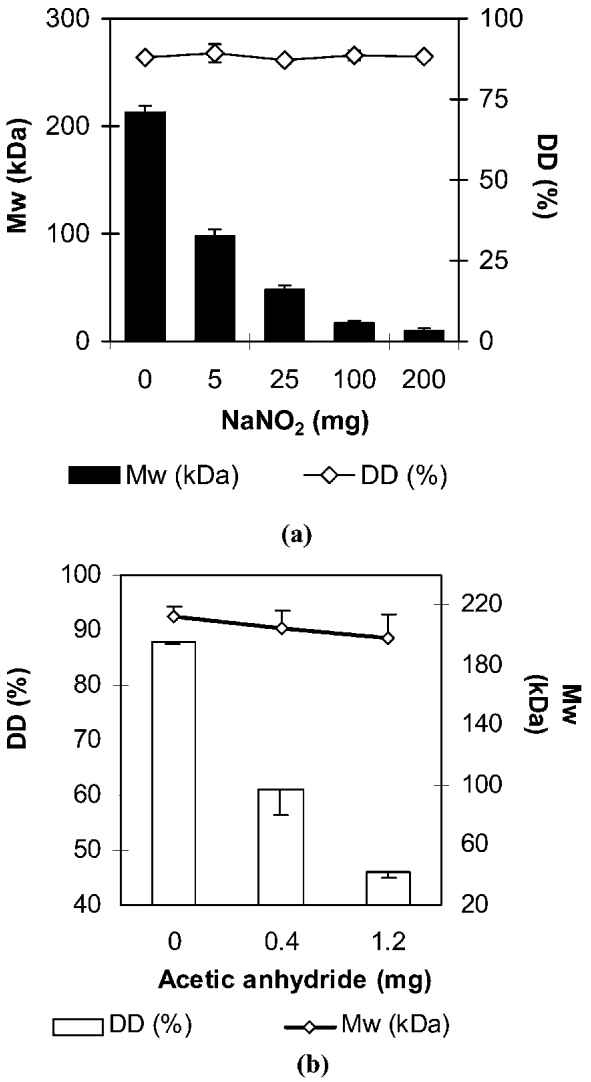

Fig. 1. Molecular weight and degree of deacetylation of chitosan after chemical treatment with (a) $NaNO_2$ and (b) acetic anhydride (mean ± S.D., n = 4).

0.33), and there were considerable overlaps in their size distribution ranges (Table 1).

A549 cellular uptake of FNP at 37°C was dependent on the Mw of chitosan, the 2-h uptake of FNP-M213D88 being 1.4-fold higher than that of FNP-M48D88 ($p < 0.01$) (Fig. 3). FNP formulated with M48D88, M17D88, and M10D88 kDa did not, however, show significant differences in cellular uptake, suggesting a threshold Mw value for increasing FNP uptake. Uptake of the reacetylated chitosan nanoparticles, FNP-M213D61 and FNP-M213D46, were 26% and 30% lower, respectively, compared to that of the parent polymer, FNP-M213D88 (Fig. 3). In contrast, the uptake of soluble FCS molecules by the A549 cells did not show any significant dependence on the Mw of the polymer in the range of 213 to 10 kDa, although a lowering of the DD from 88% to 46% led to lower FCS uptake (Fig. 3). Uptake of FCS was generally lower than that of FNP prepared from the same chitosan sample, and this difference in uptake between FCS and FNP was statistically significant for M213D88, M98D88, and M48D88.

Uptake of FNP for all the chitosan samples was linear with time for up to 4 h. Rate of uptake increased with FNP loading concentration in the range of 0.2 to 1 mg/ml (Fig. 4), with FNP-M213D88 exhibiting a greater concentration-dependent uptake than its depolymerized and reacetylated analogues. Rate of uptake plotted against concentration (Fig. 5a) shows a leveling off of FNP uptake at about 1 mg/ml, and the uptake data gave a good fit when transformed into the Michaelis-Menten type equation (Table II). K_m increased from 1.55 to 10.65 μM, and V_{max} decreased from 27.03 to 14.86 μg/mg/h, indicating lower binding affinity and uptake capacity, respectively, for FNP of decreasing Mw from 213 to 48 kDa. Lowering the Mw from 17 to 10 kDa did not produce further changes in the K_m and V_{max} values. The reacetylated FNP also exhibited increased K_m and decreased V_{max} values compared with the parent FNP (Table II), the changes in the K_m value being greater than that brought about by depolymerization.

Cellular uptake of FCS for all the chitosan samples was also linear with time for up to 4 h, but the rate of uptake of FCS increased linearly with loading concentration and did not exhibit saturation in the concentration range studied (Fig. 5b). Comparable degrees of uptake were observed of the FCS of M213D88, M98D88, and M48D88, and they were higher than the FCS uptake of M10D88, M213D61, and M213D46.

Trypan blue (TB) is commonly used at a concentration of 1% to determine cell viability because of its exclusion by viable cells. This property, combined with its capacity to quench the fluorescence of FITC (23,24), has been exploited to differentiate between extracellularly associated FITC-chitosan and FITC-chitosan internalized by viable cells (5). A similar technique was applied in this study, and Fig. 6 shows the confocal images of the A549 cells before and after post-uptake incubation with TB.

A549 cells incubated with FNP-M213D88 and FNP-M10D88 (Fig. 6a1,6a2) showed strong fluorescence, corroborating the uptake data obtained for the samples. Postuptake incubation of the cells with TB significantly reduced the fluorescent signals (Fig. 6a2,6b2), suggesting that most of the signals were located extracellularly. There was nevertheless a fair amount of fluorescence remaining in the cells after treatment with TB, particularly for cells incubated with the FNP-M213D88. The location of the signals in Fig. 6a2 and 6b2 further suggests that the FNP-M213D88 and FNP-M10D88 were not only internalized into the cytoplasm but also into the cell nucleus. For the reacetylated chitosan sample, FNP-M213D46 (Fig. 6c1,6c2), less fluorescent signals were apparent after TB incubation compared with FNP-M213D88.

A549 cells incubated with FCS-M213D88, FCS-M10D88, and FCS-M213D46 also showed strong fluorescence before TB incubation (Fig. 6d1,6e1,6f1, respectively). Unlike cells incubated with the FNP, however, hardly any fluorescent signals were apparent in these cells following TB incubation (Fig. 6d2,6e2,6f2), indicating that the cell-associated FCS-M213D88, FCS-M10D88, and FCS-M213D46 were bound extracellularly.

Effects of Mw and DD on the Cytotoxicity of NP and CS on A549 Cells

The cytotoxicity of chitosan as soluble molecules (CS) and condensed nanoparticles (NP) was evaluated as a func-

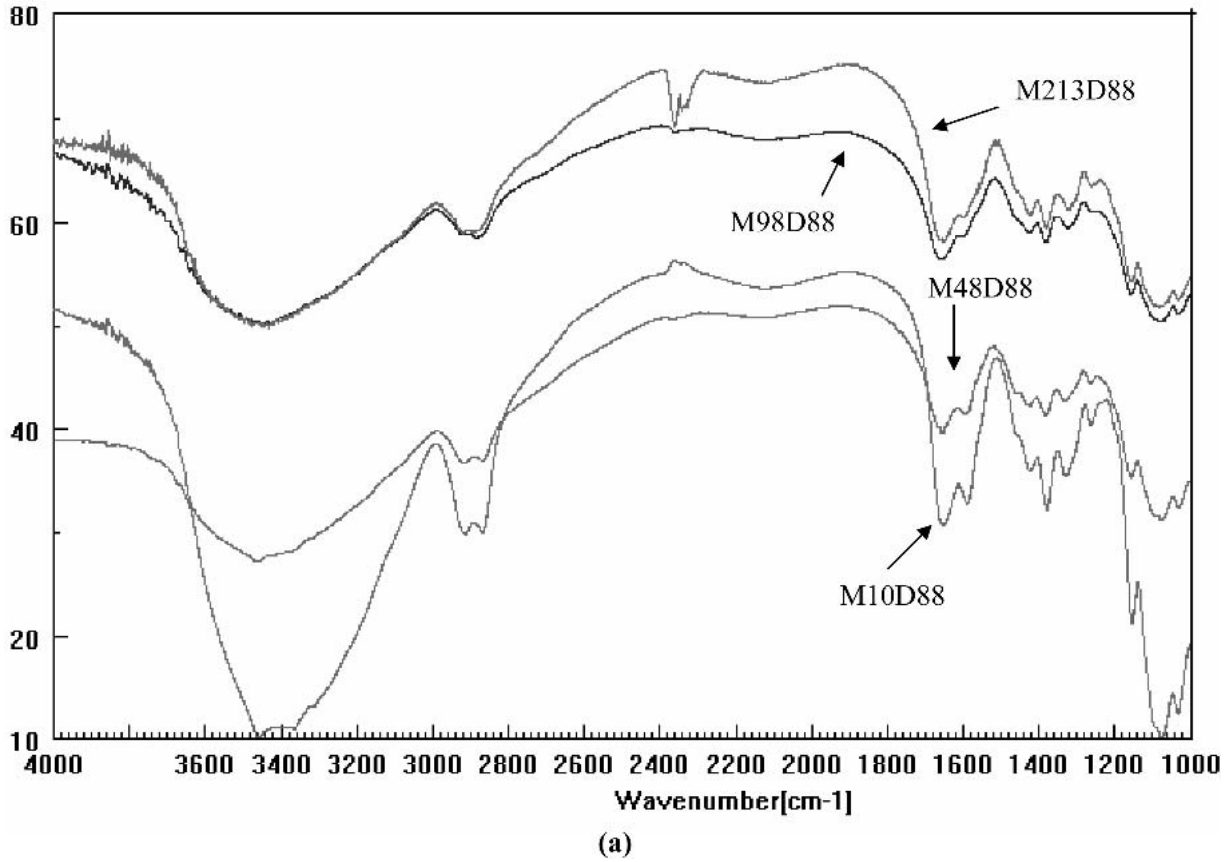

(a)

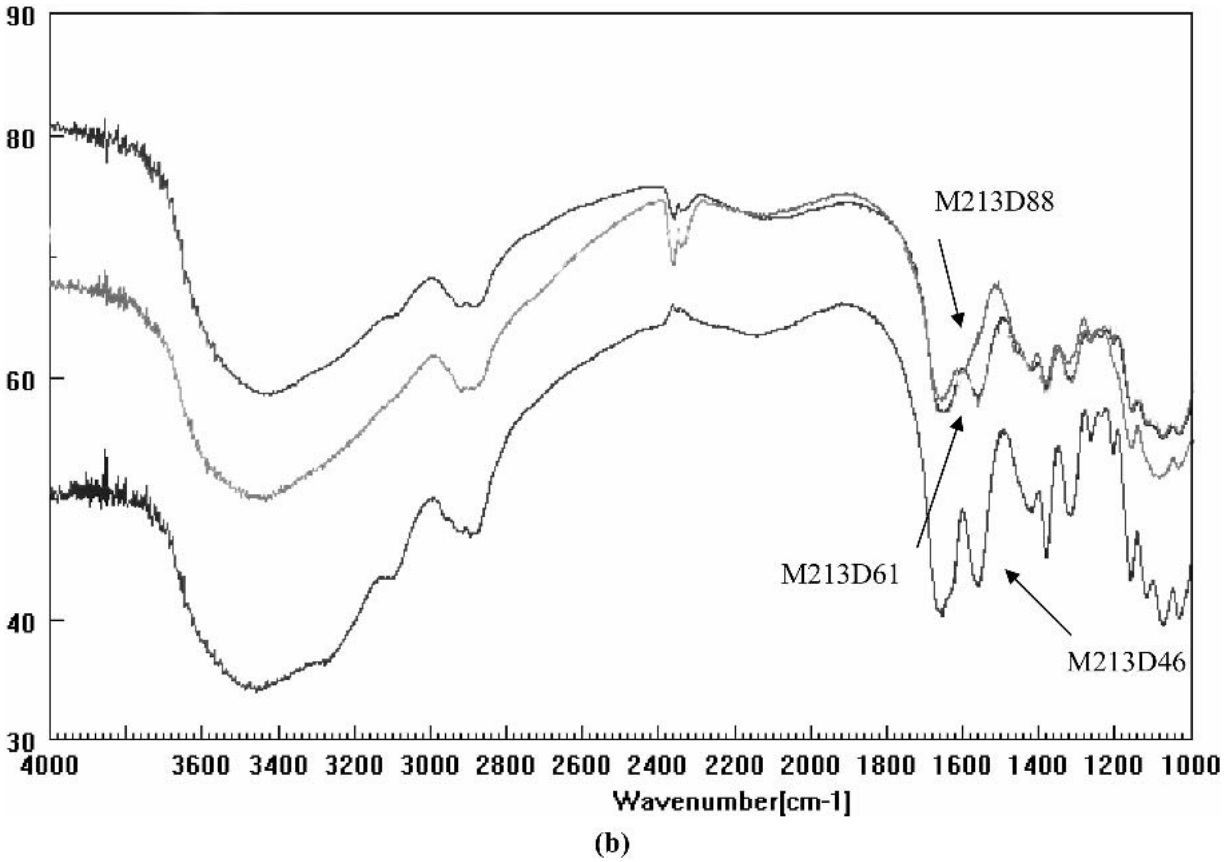

(b)

Fig. 2. Effects of (a) molecular weight and (b) degree of deacetylation on the FTIR spectrum of chitosan.

Table I. Characteristics of Chitosan Nanoparticles Prepared with Unlabeled Chitosan (NP) and FITC-Labeled Chitosan (FNP) of Different Molecular Weights and Degrees of Deacetylation

	NP					FITC labeling efficiency (w/w)	FNP				
Chitosan	Mean size	Size range	Polydispersity	ζ potential	Count rate (kcps)		Mean size	Size range	Polydispersity	ζ potential	Count rate (kcps)
M213D88	188 (12)	163–249	0.43 (0.14)	34.6 (2.1)	117.9 (2.9)	2.3	214 (10)	192–298	0.36 (0.12)	32.2 (1.8)	118.7 (3.4)
M98D88	159 (10)	135–233	0.33 (0.16)	30.5 (1.7)	104.5 (2.5)	3.4	189 (10)	152–244	0.42 (0.15)	29.7 (1.4)	111.7 (1.8)
M48D88	155 (9)	121–250	0.45 (0.17)	28.8 (2.2)	99.0 (0.4)	4.8	129 (6)	112–253	0.47 (0.18)	26.4 (2.7)	97.6 (4.7)
M17D88	122 (5)	109–201	0.50 (0.19)	26.5 (2.4)	92.2 (22.2)	7.0	110 (5)	121–234	0.52 (0.21)	25.8 (1.9)	92.8 (6.9)
M10D88	265 (8)	212–315	0.59 (0.21)	25.4 (1.3)	172.4 (13.6)	8.6	292 (7)	235–337	0.59 (0.21)	24.9 (1.9)	185.8 (8.5)
M213D61	258 (18)	224–319	0.51 (0.16)	15.4 (2.1)	87.4 (5.8)	4.0	268 (29)	222–350	0.46 (0.14)	12.1 (1.9)	92.4 (3.7)
M213D46	341 (74)	247–387	0.51 (0.17)	14.3 (3.2)	74.8 (4.7)	5.7	333 (87)	251–394	0.49 (0.15)	11.4 (1.7)	86.4 (4.3)

Values in parentheses represent S.D. (n = 3).

tion of Mw, DD, and concentration. CS and NP formulated with chitosans of DD 88% and Mw ranging from 213 to 10 kDa showed comparable dose-dependent cytotoxicity in the concentration range of 0.098 to 1.667 mg/ml as measured by the MTT assay (Fig. 7a,b). Cell viability was generally not affected by CS and NP at concentrations lower than 0.741 mg/ml but showed a progressive decline when exposed to increasing concentrations beyond 0.741 mg/ml. Reacetylation of chitosan significantly improved the cytotoxicity profiles of the CS and NP. Although CS-M213D88 and NP-M213D88 yielded less than 10% cell viability at a concentration of 1.667 mg/ml, cells exposed to equivalent concentrations of CS and NP prepared with M213D61 and M213D46 retained 60% viability (Fig. 7c,d). The neutral red uptake assay gave comparable CS and NP cytotoxicity profiles (not shown) to the MTT assay.

Figure 7 shows the IC_{50} and IC_{20} values calculated from the cell viability–concentration graphs. CS and NP from the same chitosan sample did not yield significantly different IC_{50} and IC_{20} values. Reducing the chitosan Mw from 213 to 10 kDa also did not change the IC_{50} and IC_{20} values for the CS and NP samples (Fig. 8a,b), with the mean IC_{50} values remaining within the narrow range of 1.1 to 1.2 mg/ml for the MTT assay (1.3 to 1.5 mg/ml for the neutral red assay). However, when DD of the polymer was decreased from 88% to 61%, the IC_{50} value for the NP as determined by the MTT assay was found to increase by 1.7-fold, from 1.2 to 2.0 mg/ml (Fig. 8c). A further decrease in the DD to 46% produced a modest rise in the IC_{50} value to 2.2 mg/ml. Parallel trends were observed for the CS samples (Fig. 8c), and data from the neutral red assay supported these findings (Fig. 8d).

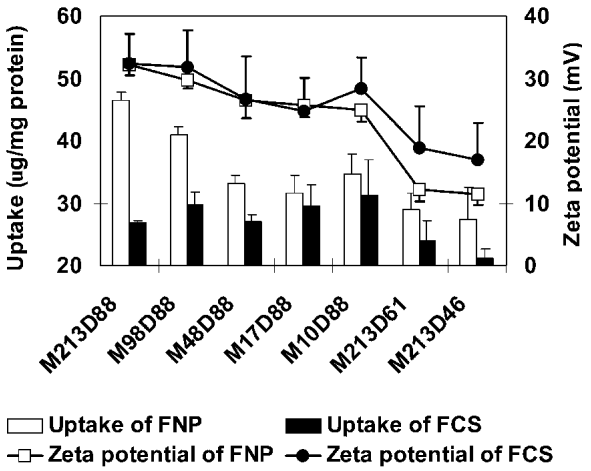

Fig. 3. Effects of chitosan molecular weight and degree of deacetylation on the 2-h uptake of FITC-chitosan nanoparticles and FITC-chitosan molecules by A549 cells at 37°C. The ζ potential was evaluated at a concentration of 0.5 mg/ml in HBSS-HEPES solution. (Data expressed as mean ± S.D., n = 4.)

DISCUSSION

The dependence of FNP cellular uptake on the chitosan Mw and DD might be related to the size and ζ potential of the nanoparticles. Cellular uptake of polymer nanoparticles has been reported to be influenced by particle size, the intestinal uptake of polystyrene and poly(lactic-co-glycolic acid) particles of 100 nm being significantly greater than those of corresponding particles of 500 and >1000 nm diameter (25,26). However, particle size does not appear to be the dominant factor influencing the uptake of FNP by the A549 cells. This is because FNP-M17D88 did not exhibit the highest cellular uptake despite having the smallest mean particle size of 110 nm. Neither did it show a significantly different uptake from FNP-M10D88, which was 2.6-fold larger in mean diameter. Moreover, the FNP were polydisperse in size and, although the batches differ significantly in mean particle size, they contained a considerable number of particles in the same size range.

The decrease in mean size of the chitosan nanoparticles with decreasing polymer Mw in the range of 213 to 17 kDa was expected and could be attributed to shorter polymer chains giving rise to smaller nanoparticles. However, nanoparticles of the shortest chitosan chain, M10D88, were unex-

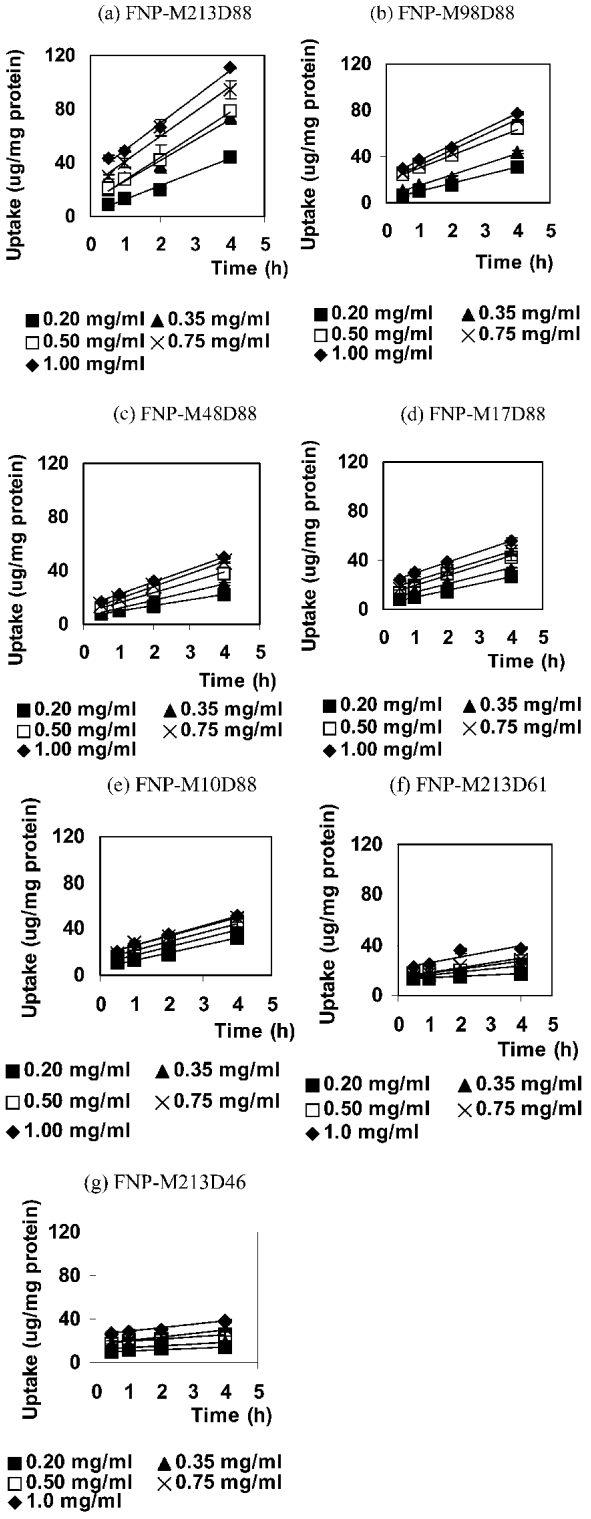

Fig. 4. Uptake of FITC-chitosan nanoparticles as a function of loading concentration by A549 cells at 37°C. (Data expressed as mean ± S.D., n = 3): (a) M213D88, (b) M98D88, (c) M48D88, (d) M17D88, (e) M10D88, (f) M213D61, and (g) M213D46.

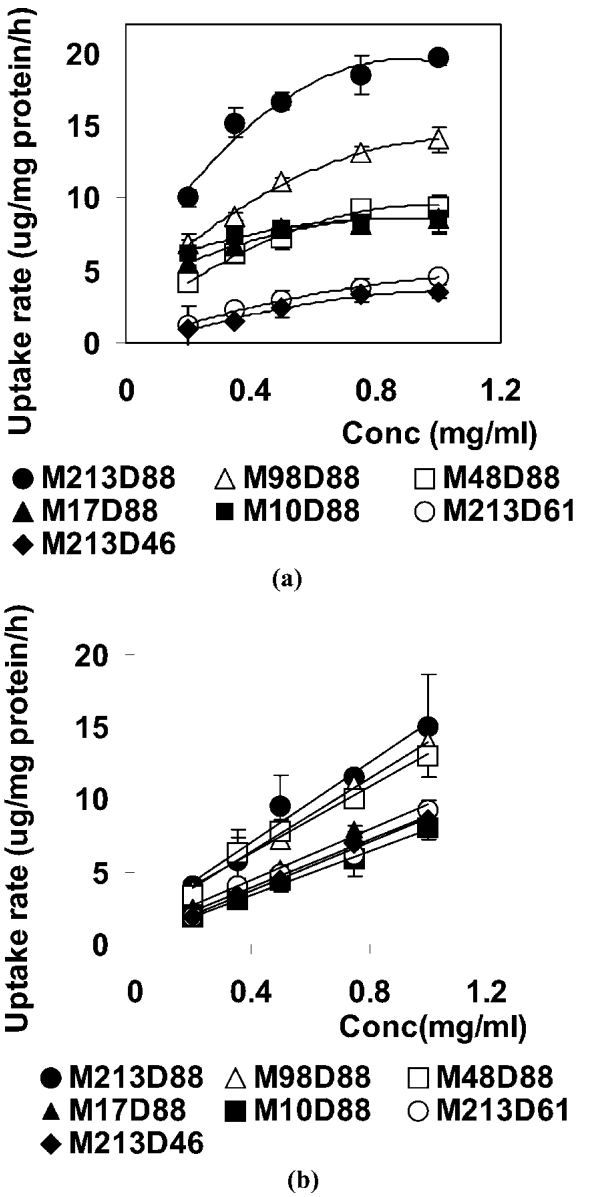

Fig. 5. Rate of uptake of (a) FITC-chitosan nanoparticles, (b) FITC-chitosan molecules by A549 cells following 4 h of incubation at 37°C at various dosing concentrations. (Data expressed as mean ± S.D., n = 3.)

pectedly larger than those produced from chitosans of higher Mw. The mechanism is not known, but the larger particles did not arise from particle agglomeration, as indicated by the TEM micrographs. The reacetylated chitosans also gave rise to larger nanoparticles. In these cases, the smaller number of amino functional groups could have reduced the capacity of the chitosan chains for ionotropic gelation with TPP, and the resultant smaller degree of deswelling led to larger particles being produced.

The FNP uptake data correlate better with the ζ potential data, as can be seen from Fig. 3. The reduced uptake of FNP-M48D88, compared with the parent FNP-M213D88, was in line with its lower ζ potential (26 mV vs. 32 mV), whereas FNP-M48D88, FNP-M17D88, and FNP-M10D88 had comparable ζ potentials and showed similar cellular uptake. The smaller ζ potential of the reacetylated FNP was also accompanied by lower cellular uptake, although the uptake was not as low as predicted from the ζ potential. The combined data support our hypothesis (4) that the uptake of chitosan nanoparticles by A549 cells was initiated by electrostatic interac-

Table II. Effects of Chitosan Molecular Weight and Degree of Deacetylation on the Uptake Kinetics Parameters for Chitosan Nanoparticles

Chitosan sample	Uptake kinetic parameters for chitosan nanoparticles		
	K_m (μM)	V_m (μg/mg/h)	R^2
M213D88	1.55	27.03	0.9734
M98D88	3.62	18.76	0.9973
M48D88	10.65	14.86	0.9946
M17D88	10.11	10.17	0.986
M10D88	10.89	9.61	0.9951
M213D61	11.61	16.92	0.9925
M213D46	14.95	15.9	0.9872

R^2 represents the goodness of fit of the uptake data to the Michaelis-Menten type equation.

tions between the nanoparticles and the cell membrane. FNP with a higher ζ potential would exhibit a stronger affinity for the negatively charged cell membrane (27,28), accounting for its higher cellular uptake.

Interbatch variation in nanoparticle concentration might also account for the disparity in uptake among the various FNPs. The count rate, which reflects the concentration of particles in a sample (Table I), suggests that the ionotropic gelation of M10D88 with TPP yielded a much higher number of nanoparticles on a weight basis compared to the other chitosan samples. Thus, a favorable particle concentration gradient might have contributed to the FNP-M10D88 having a comparable cellular uptake with the FNP-M48D88 and FNP-M17D88 despite its relatively larger size distribution.

FNP uptake was a saturable event for all the chitosan samples evaluated. The intracellular fluorescent signals obtained after postuptake TB incubation supported the hypothesis that the FNP was endocytosed. This internalization was evident even for FNP prepared with chitosans of low Mw of 10 kDa, or low DD of 46%. The decrease in binding affinity and uptake capacity for FNP prepared with chitosans of decreasing Mw and DD again indicated that the endocytic event was preceded by electrostatic interactions between the FNP and the cellular membrane (28).

In contrast, the cellular uptake of FCS did not show saturation (Fig. 5b) and was not dependent on the chitosan Mw, probably because depolymerization did not significantly modify the ζ potential of FCS (Figs. 2 and 4). Decreasing the chitosan DD to 61% and 46% caused the ζ potential to drop to 18.9 ± 6.6 mV and 16.9 ± 5.9 mV, respectively, which resulted in the decreased uptake of the reacetylated FCS. Pos-

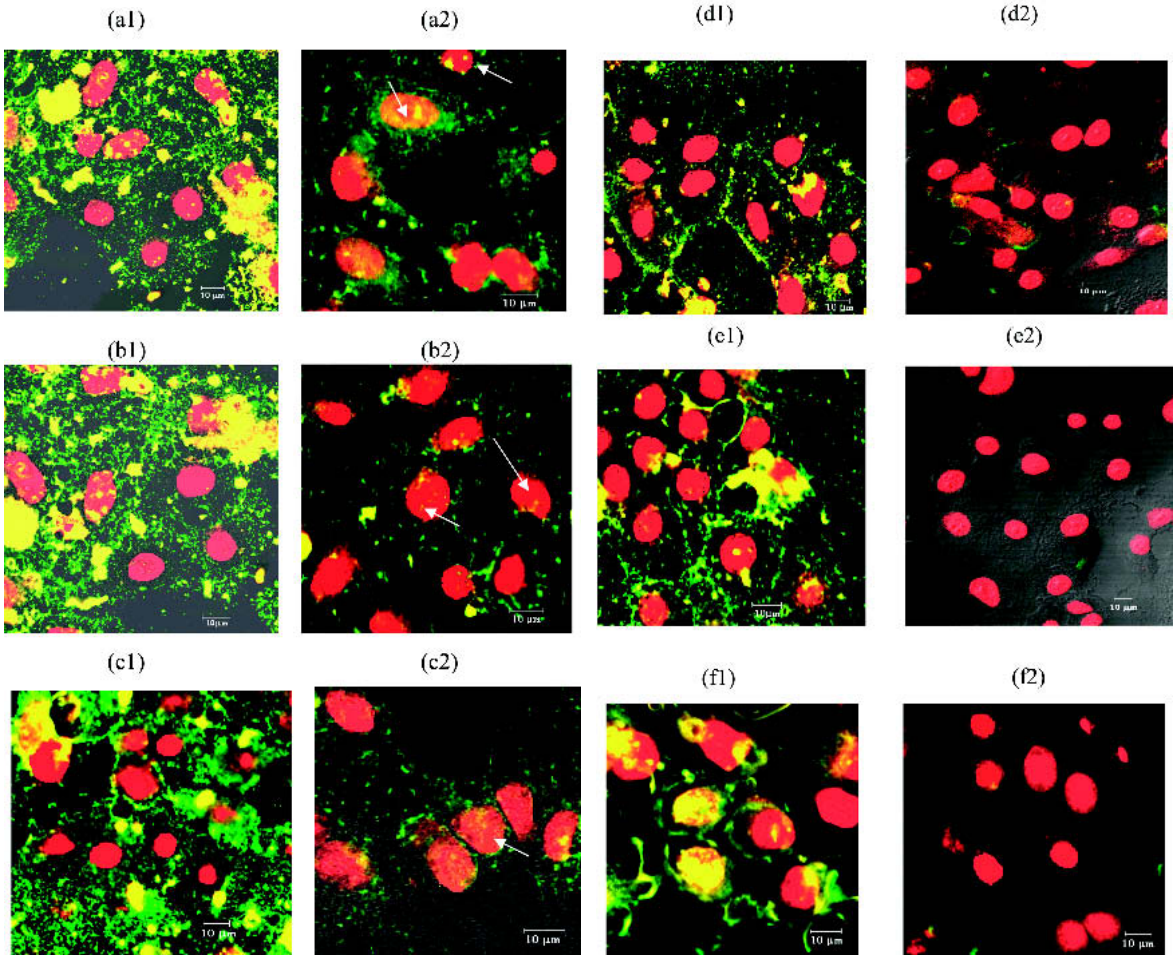

Fig. 6. Confocal images of A549 cells coincubated with (a) FNP-M213D88, (b) FNP-M10D88, (c) FNP-M213D46, (d) FCS-M213D88, (e) FCS-M10D88, and (f) FCS-M213D46 for 2 h before (1) and after (2) postuptake incubation with 400 μg/ml of trypan blue solution.

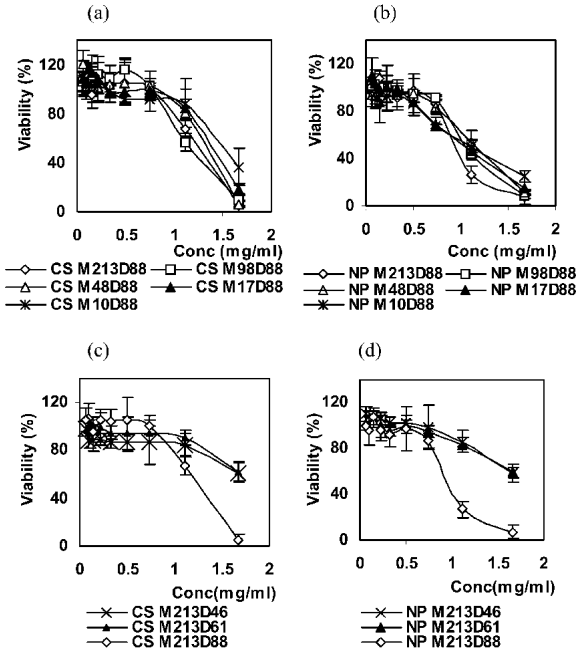

Fig. 7. *In vitro* cytotoxicity of chitosan nanoparticles (NP) and chitosan solutions (CS) on A549 cells as measured by the MTT assay. Cell viability is expressed as mean ± S.D. (n = 8): (a) solutions of chitosan with different molecular weights; (b) nanoparticles of chitosan with different molecular weights; (c) solutions of chitosan with different degrees of deacetylation; (d) nanoparticles of chitosan with different degrees of deacetylation.

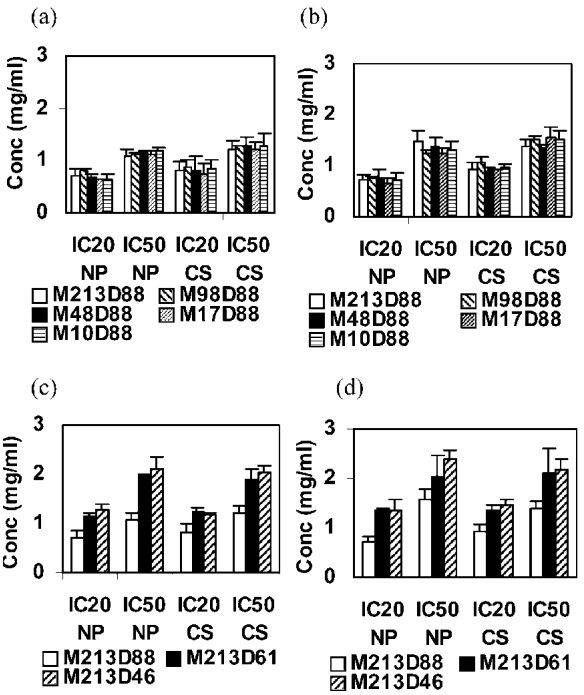

Fig. 8. Effects of chitosan molecular weight and degree of deacetylation on the IC_{50} (mg/ml) and IC_{20} (mg/ml) values of chitosan molecules (CS) and nanoparticles (NP) as determined by the MTT assay (a, c) and the neutral red uptake assay (b, d) (mean ± S.D., n = 3).

tuptake quenching by TB suggested that the cell-associated FCS from all chitosan samples was located extracellularly; i.e., the chitosan molecules were not endocytosed following mucoadhesion. Moreover, the data indicated that the different mechanisms of interaction between the adsorptive cells and chitosan presented as soluble molecules and as condensed nanoparticles were not modified by reducing the polymer Mw from 213 to 10 kDa or by lowering the polymer DD from 88% to 46%.

A comparison of the cytotoxicity and uptake data suggests that cellular uptake of CS and NP was not associated with their cytotoxicity. Unlike the uptake data, there was no difference in cytotoxicity between CS and NP toward the A549 cells. Both chitosan entities exhibited significant cytotoxicity only at concentrations higher than 0.741 mg/ml, the cytotoxicity not being significantly reduced by a lowering of the polymer Mw to 10 kDa. On the other hand, decreasing the DD of the polymer from 88% to 61% was found to attenuate the cytotoxicity of CS and NP to comparable degrees. The disparity could be attributed to the smaller effect of Mw on the ζ potential of CS and NP compared with changes in DD. Our data are in agreement with reports that the cytotoxicity of cationic polymers, such as poly-L-lysine, poly-L-arginine, and protamine, was directly related to their surface charge density (29,30). Although the number of primary amino groups was important (31,32), the charge density resulting from the number of groups and the three-dimensional arrangement of the cationic residues were also important contributors of cytotoxicity for a material. Chitosans with high degrees of deacetylation have extended conformation because of charge repulsion, which might allow them to bind more readily to cell membranes than coiled chitosans of lower degrees of deacetylation.

CONCLUSIONS

Transformation of chitosan into nanoparticles did not modify the cytotoxicity profile of the polymer but facilitated its endocytosis by A549 cells. The nanoparticle uptake was a saturable event for chitosan samples with Mw ranging from 213 to 10 kDa and with DD ranging from 88% to 46%. Mw and DD affected the uptake efficiency by modulating the ζ potential of the chitosan nanoparticles, with the binding affinity and uptake capacity for the nanoparticles decreasing with decreasing chitosan Mw and DD. In comparison, uptake of chitosan molecules did not exhibit saturation kinetics and was dependent on the polymer DD but not Mw. Both chitosan molecules and nanoparticles exhibited comparable cytotoxicity, yielding similar IC_{50} and IC_{20} values when evaluated against the A549 cells. Cytotoxicity of both chitosan entities was attenuated by decreasing polymer DD but was less affected by a lowering in Mw.

ACKNOWLEDGMENTS

This study was supported by a National University of Singapore grant (R148-000-045-112). Min Huang is grateful to the National University of Singapore for financial support for her graduate studies.

REFERENCES

1. K. A. Janes, M. P. Fresneau, A. Marazuela, A. Fabra, and M. J. Alonso. Chitosan nanoparticles as delivery systems for doxorubicin. *J. Control. Rel.* **73**:255–267 (2001).

2. H.-Q. Mao, K. Roy, V. L. Troung-Le, K. A. Janes, K. Y. Lin, Y. Wang, J. T. August, and K. W. Leong. Chitosan-DNA nanoparticles as gene carriers: synthesis, characterization and transfection efficiency. *J. Control. Rel.* **70**:399–421 (2001).
3. L. Illum, I. Jabbal-Gill, M. Hinchcliffe, A. N. Fisher, and S. S. Davis. Chitosan as a novel nasal delivery system for vaccines. *Adv. Drug Deliv. Rev.* **51**:81–96 (2001).
4. M. Huang, Z. S. Ma, E. Khor, and L.-Y. Lim. Uptake of FITC-chitosan nanoparticles by A549 cells. *Pharm. Res.* **19**:1488–1494 (2002).
5. Z. S. Ma and L.-Y. Lim. Uptake of chitosan and associated insulin in the Caco-2 cell monolayers: a comparison between chitosan molecules and chitosan nanoparticles. *Pharm. Res.* **20**:1812–1819 (2003).
6. H. S. Blair, J. Guthrie, T. K. Law, and P. Turkington. Chitosan and modified chitosan membranes. I. Preparation and characterization. *J. Appl. Polym. Sci.* **33**:641–656 (1987).
7. K. M. Vårum, M. M. Mhyr, R. J. N. Hjerde, and O. Smidsrød. *In vitro* degradation rates of partially N-acetylated chitosans in human serum. *Carbohydr. Res.* **299**:99–101 (1997).
8. E. Khor. *Chitin: Fulfilling a Biomaterials Promise.* Elsevier Science, Oxford, UK (2001).
9. D. F. Williams. Progress in biomedical engineering. 4. Definitions in biomaterials. In: Williams, D.F. Editor. *Proceedings of a Consensus Conference of the European Society for Materials, Chester, UK.* Elsevier, Amsterdam. (1987).
10. K. Y. Lee, W. S. Ha, and H. L. Park. Blood compatibility and biodegradability of partially N-acetylated chitosan derivatives. *Biomaterials* **16**:1211–1216 (1995).
11. K. Tomihata and Y. Ikada. *In vitro* and *in vivo* degradation of films of chitin and its deacetylated derivatives. *Biomaterials* **18**: 567–575 (1997).
12. H. Zhang and S. H. Neau. *In vitro* degradation of chitosan by a commercial enzyme preparation: effect of molecular weight and degree of deacetylation. *Biomaterials* **22**:1653–1658 (2001).
13. B. Carreño-Gómez and R. Duncan. Evaluation of the biological properties of soluble chitosan and chitosan microspheres. *Int. J. Pharm.* **148**:231–240 (1997).
14. N. G. M. Schipper, K. M. Vårum, and P. Artursson. Chitosans as absorption enhancers for poorly absorbable drugs.1: influence of molecular weight and degree of acetylation on drug transport across human intestinal epithelial (Caco-2) cells. *Pharm. Res.* **13**: 1686–1691 (1996).
15. Q.P. Peniston and E. L. Johnson. Process for depolymerization of chitosan. US Patent 3,922,260, November 25, 1975.
16. S. Hirano, Y. Kondo, and K. Fujii. Preparation of acetylation derivatives of modified chito-oligosaccharides by the depolymerisation of partially N-acetylated chitosan with nitrous acid. *Carbohydr. Res.* **144**:338–341 (1985).
17. P. Calvo, C. Remuñán-López, J. L. Vila-Jato, and M. J. Alonso. Novel hydrophilic chitosan-polyethylene oxide nanoparticles as protein carriers. *J. Appl. Polym. Sci.* **63**:125–132 (1997).
18. D. J. Giard. *In vitro* cultivation of human tumors: establishment of cell lines derived from a series of solid tumors. *J. Natl. Cancer Inst.* **51**:1417–1423 (1973).
19. T. Mosmann. Rapid colorimetric assay for cellular growth and survival: application to proliferation and cytotoxicity. *J. Immunol. Methods* **65**:55–63 (1983).
20. E. Borenfreund and J. A. Puerner. Toxicity determined *in vitro* by morphological alterations and neutral red absorption. *Toxicol. Lett.* **24**:119–124 (1985).
21. S. C. Tan. *A study on the isolation and characterization of fungal chitosan.* Thesis (M.Sc.), School of Biological Sciences, Faculty of Science, National University of Singapore (1998).
22. S. C. Tan, E. Khor, T. K. Tan, and S. M. Wong. The degree of deacetylation of chitosan: advocating the first derivative UV-spectrophotometry method of determination. *Talanta* **45**:713–719 (1998).
23. C. P. Wan, C. S. Park, and B. H. S. Lau. A rapid and simple microfluorometric phagocytosis assay. *J. Immunol. Methods* **162**: 1–7 (1993).
24. S. Sahlin, J. Hed, and I. Rundquist. Differentiation between attached and ingested immune complexes by a fluorescence quenching cytofluorometric assay. *J. Immunol. Methods* **60**:115–124 (1983).
25. T. Jung, W. Kamm, A. Breitenbach, E. Kaiserling, J. X. Xiao, and T. Kissel. Biodegradable nanoparticles for oral delivery of peptides: is there a role for polymers to affect mucosal uptake? *Eur. J. Pharm. Biopharm.* **50**:147–160 (2000).
26. P. Jani, D. E. McCarthy, and A. T. Florence. Nanosphere and microsphere uptake via Peyer's patches: observation of the rate of uptake in the rat after a single oral dose. *Int. J. Pharm.* **86**: 239–246 (1992).
27. M. D. Hughes, M. Hussain, Q. Nawaz, P. Sayyed, and S. Akhtar. The cellular delivery of antisense oligonucleotides and ribozymes. *Drug Discov. Today* **6**:303–315 (2001).
28. Y. Yasuomi, S. Kazuya, N Makiya, Y. Fumiyoshi, Y. Kiyoshi, H. Mitsuru, and T. Yoshinobu. Pharmacokinetic analysis of *in vivo* disposition of succinylated proteins targeted to liver nonparenchymal cells via scavenger receptors: Importance of molecular size and negative charge density for *in vivo* recognition by receptors. *J. Pharmacol. Exp. Ther.* **301**:467–477 (2002).
29. S. W. Chang, J. Y. Westcott, J. E. Henson, and N. F. Voelkel. Pulmonary vascular injury by polycations in perfused rat lungs. *J. Appl. Physiol.* **62**:1932–1943 (1987).
30. H. M. Ekrami and W. C. Shen. Carbamylation decreases the cytotoxicity but not the drug-carrier properties of polylysines. *J. Drug Target.* **2**:469–475 (1995).
31. L. Dekie, V. Toncheva, P. Dubruel, E. H. Schacht, L. Barrett, and L. W. Seymour. Poly-L-glutamic acid derivatives as vectors for gene therapy. *J. Control. Rel.* **65**:187–202 (2000).
32. P. Ferruti, S. Knobloch, E. Ranucci, R. Duncan, and E. Gianasi. A novel modification of poly(L-lysine) leading to a soluble cationic polymer with reduced toxicity and with potential as a transfection agent. *Macromol. Chem. Phys.* **199**:2565–2575 (1998).